Phys. Status Solidi A **211**, No. 1, 27–33 (2014) / **DOI** 10.1002/pssa.201330092

Part of Topical Section on
Emerging Semiconducting Oxides

physica status solidi a
www.pss-a.com
applications and materials science

Homoepitaxial growth of β-Ga_2O_3 layers by metal-organic vapor phase epitaxy

Guenter Wagner[*,1], Michele Baldini[1,2], Daniela Gogova[1], Martin Schmidbauer[1], Robert Schewski[1], Martin Albrecht[1], Zbigniew Galazka[1], Detlef Klimm[1], and Roberto Fornari[1,†]

[1] Leibniz Institute for Crystal Growth, Max-Born-Str. 2, 12489 Berlin, Germany
[2] CNR-IMEM, Parco Area delle Scienze 37/A, 43124 Parma, Italy

Received 1 July 2013, revised 3 September 2013, accepted 3 September 2013
Published online 3 October 2013

Keywords Ga_2O_3, metal-organic vapor phase epitaxy, structure, thin films, transparent semiconducting oxides

[*] Corresponding author: e-mail guenter.wagner@ikz-berlin.de, Phone: +49 30 63922846, Fax: +49 30 63923003
[†] Present address: Department of Physics and Earth Sciences, University of Parma, Viale delle Scienze 7/A, 43124 Parma, Italy.

Epitaxial β-Ga_2O_3 layers have been grown on β-Ga_2O_3 (100) substrates using metal-organic vapor phase epitaxy. Trimethylgallium and pure oxygen or water were used as precursors for gallium and oxygen, respectively. By using pure oxygen as oxidant, we obtained nano-crystals in form of wires or agglomerates although the growth parameters were varied in wide range. With water as an oxidant, smooth homoepitaxial β-Ga_2O_3 layers were obtained under suitable conditions. Based on thermodynamical considerations of the gas phase and published *ab initio* data on the catalytic action of the (100) surface of β-Ga_2O_3 we discuss the adsorption and incorporation processes that promote epitaxial layer growth. The structural properties of the β-Ga_2O_3 epitaxial layers were characterized by X-ray diffraction pattern and high resolution transmission electron microscopy. As-grown layers exhibited sharp peaks that were assigned to the monocline gallium oxide phase and odd reflections that could be assigned to stacking faults and twin boundaries, also confirmed by TEM. Shifts of the layer peak towards smaller 2θ values with respect to the Bragg reflection for the bulk peaks have been observed. After post growth thermal treatment in oxygen-containing atmosphere the reflections of the layers do shift back to the position of the bulk β-Ga_2O_3 peaks, which was attributed to significant reduction of lattice defects in the grown layers after thermal treatment.

© 2013 WILEY-VCH Verlag GmbH & Co. KGaA, Weinheim

1 Introduction Metal oxides like Ga_2O_3, In_2O_3, SnO_2, and ZnO are transparent conducting oxides (TCO) of high industrial relevance which have been widely applied for fabrication of transparent electrodes in photovoltaic devices, liquid crystal displays, light emitting diodes, and chemical sensors [1–3]. For such applications, thin oxide films just need to be highly conductive and transparent but in principle they do not require good structural perfection. Indeed they have an amorphous or polycrystalline structure and a relatively high level of defects.

Recently, there is a great interest in considering these metal oxides from another point of view, namely as wide band gap transparent semiconducting oxides (TSOs). That means there are numerous attempts to obtain single-crystalline thin oxide films with good crystallographic properties and controlled carrier concentration. When grown as single crystalline epitaxial films, as it is normally done for classical semiconductors (e.g. Si, GaAs, InP), they could offer the great potential of a new class of semiconductors, with application in transparent microelectronics, optoelectronics, power electronics, short wavelength photonics as well as chemical and biological sensor devices [4–8].

Monoclinic β-Ga_2O_3 is a material with a band gap E_g of 4.9 eV and high transparency in the visible and deep-UV region. When pure, undoped, and stoichiometric it is an electrical insulator due to its large band gap.

Up to now, thin films of β-Ga_2O_3, were generally deposited on substrates such as Al_2O_3, Si, GaAs, TiO_2, ZrO_2:Y, MgO [9–14] because native substrates prepared from bulk crystals with identical composition and crystal structure are not commercially available. Heteroepitaxial deposition processes result in polycrystalline layers with a very high density of extended defects due to differences in lattice symmetry and the large lattice mismatch between layer and substrates.

Heteroepitaxial β-Ga_2O_3 films were grown by various methods: physical vapor deposition, molecular-beam epitaxy [9, 10], pulsed laser deposition [11, 12], electron-beam evaporation [13], and metal-organic chemical vapor deposition [15, 17, 18]. On the other hand, step-flow deposition of

© 2013 WILEY-VCH Verlag GmbH & Co. KGaA, Weinheim

homoepitaxial β-Ga_2O_3 thin layers was demonstrated by plasma-assisted MBE [16]. It is expected that the homo-epitaxial growth by metal-organic vapor phase epitaxy (MOVPE) will provide β-Ga_2O_3 films of improved crystalline quality, since the growth takes place at thermodynamical conditions closer to equilibrium as compared with other thin film growth techniques.

In the following, we report on homoepitaxial growth of single phase, smooth β-Ga_2O_3 layers. We investigated the effects of two alternative oxygen sources, namely O_2 and H_2O on the initial stage of crystal growth and on the properties of the grown layers.

2 Experimental The epitaxial growth of β-Ga_2O_3 was carried out in a commercial vertical MOVPE reactor (SMI inc., USA) at low pressure conditions. Trimethylgallium (TMGa) was used as gallium precursor, pure oxygen and alternatively H_2O as oxygen sources and high purity Ar as a carrier gas. The temperature of the TMGa-bubbler was set between −10 and −5 °C at a pressure of 1100 mbar. The flow rates of TMGa, oxygen, and water were 5 sccm, 200–1500 sccm, and 400–1500 sccm, respectively. During layer deposition, the substrate temperature were kept in the range from 750 to 850 °C and the chamber pressures were set between 5 and 100 mbar. In dependence on the growth parameters, the resulting growth rate was 3–8 nm min^{-1}. The structural properties of the β-Ga_2O_3 layers were analyzed by means of high resolution X-ray diffraction (XRD Master HR, Seifert, Cu $K\alpha_1$ radiation) and transmission electron microscopy (aberration corrected FEI Titan 80–300 operated at 300 kV). In addition, spectroscopic ellipsometry (MM-16, Horiba Jobin Yvon), atomic force microscopy (AFM; Asylum Research MFP3D stand alone) and scanning electron microscopy (FEI Nova 600 Dual Beam) investigations were carried out in order to determine the layer thickness and to reveal the surface morphology of the epitaxial layers. Capacitance–voltage and conductivity measurements have been performed to characterize the electrical properties of the grown layers.

One side polished $1 \times 1\,cm^2$ β-Ga_2O_3 substrates were used. The high quality n-type β-Ga_2O_3 single crystals for the preparation of (100) β-Ga_2O_3 substrates were grown by the Czochralski method [19]. After solvent cleaning with acetone and isopropanol in ultrasonic bath, the substrates were annealed in oxygen atmosphere at 1000 °C for 60 min to remove the subsurface damage layer. After this process, the substrates showed a terraced surface with a step height of about 0.6 nm, corresponding to half a unit cell along the (100) direction and terrace widths of about 70–100 nm as a result of the slight deviation from the (100) orientation (generally smaller than 0.2° after final polishing). Figure 1 shows a typical AFM image of a β-Ga_2O_3 substrate surface ready for the layer deposition.

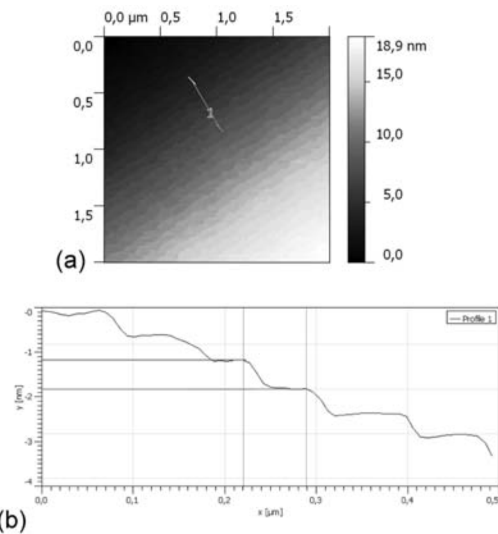

Figure 1 (a) AFM image and (b) selected line scan of a β-Ga_2O_3 (100) surface after 1 h annealing at 1000 °C in oxygen-containing environment.

3 Experimental results

3.1 β-Ga_2O_3 deposition by using trimethyl-gallium and pure oxygen In the first set of experiments, TMGa and pure oxygen were used as precursors. To prevent dissociation of the Ga_2O_3-substrate surface an oxygen flux of 400 sccm was maintained in the reactor during the heating up to the growth temperature and also during cooling down. Figure 2 shows a SEM image of a sample surface after growing for 15 min at a temperature of 775 °C and chamber pressure of 20 mbar, under Ga and oxygen fluxes of 5 and 400 sccm, respectively.

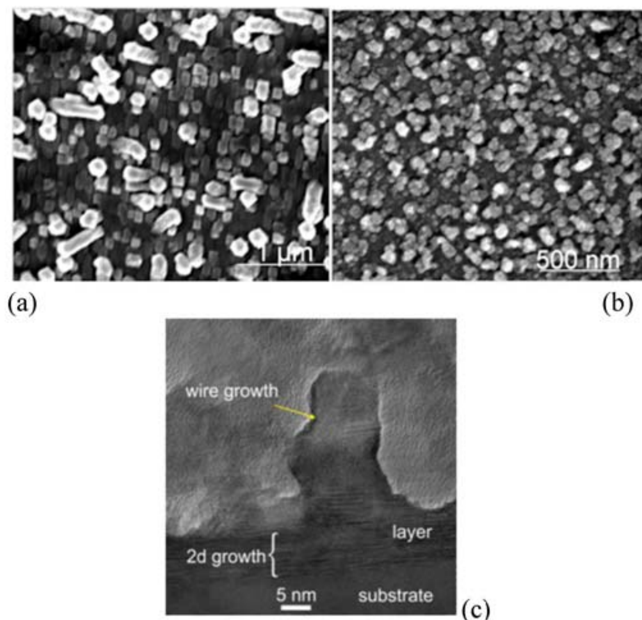

Figure 2 SEM-image of β-Ga_2O_3 crystals grown on a β-Ga_2O_3 single crystalline substrate from TMGa and pure oxygen, T_g: 775 °C, O/Ga ratio: 1200 (a), T_g: 800 °C, O/Ga ratio: 3200 (b). (c) Cross-sectional high resolution TEM image of a homoepitaxial grown β-Ga_2O_3 layer with oxygen as a precursor.

© 2013 WILEY-VCH Verlag GmbH & Co. KGaA, Weinheim

β-Ga_2O_3 deposited in the form of long wires, up to 500 nm in length and up to 100 nm in diameter, preferentially (100)-oriented (Fig. 2a). At a deposition temperature of 800 °C and increased oxygen-to-gallium ratio of 3200 the grown Ga_2O_3 material looked like an agglomeration of nanocrystals (Fig. 2b).

The TEM image shown in Fig. 2c shows a cross-section of typical wire. As can be seen in the image initially a thin layer with high densities of planar defects grows two-dimensionally. Then growth turns into wire growth. It has to be mentioned, that all wires are growing epitaxially but the coherency of the layer is lost. All attempts to deposit closed homoepitaxial layers of β-Ga_2O_3 on (100)-oriented β-Ga_2O_3 substrates using oxygen and TMG as precursors failed, although the growth parameters were varied in a wide range: substrate temperatures between 750 and 850 °C, chamber pressure between 5 and 100 mbar, and oxygen-to-gallium ratios up to 9500 were used. In all cases only β-Ga_2O_3 nanocrystals (either wires or agglomerates) were obtained, despite the use of single crystalline β-Ga_2O_3 substrates. This suggests that pure oxygen is not suitable for growth of homoepitaxial layers on β-Ga_2O_3 substrates. For this reason, we turned the attention to another source of oxygen, namely water vapor.

3.2 β-Ga_2O_3 deposition by using trimethylgallium and water as oxygen source Trimethylgallium and ultra pure water were used as precursors and Ar as the carrier gas. The temperature of the water bubbler was fixed at 50 °C and a pressure of 300 mbar.

Figure 3 shows the dependence of the measured growth rate on the deposition temperature. With increasing deposition temperature, a decrease of the growth rate was observed. This is due to formation and desorption of gallium suboxide, Ga_2O, which is formed more readily at higher temperatures. On the other hand, for the initial step of nucleation as well as for the subsequent layer growth a higher substrate temperature is desirable as it increases the species mobility on the growth interface and improves the growth kinetics. The chosen deposition temperature of 800 °C is a compromise between deposition efficiency and crystalline quality; TMGa and water fluxes were 5 and 180 sccm, respectively. After a deposition time of 30 min, a layer of about 170 nm was grown. A typical layer surface morphology as measured by SEM and AFM is shown in Fig. 4a and b, respectively. A layer roughness (rms) of 6.5 nm was evaluated. The growth rate was about 5 nm min^{-1}. The surface of the grown layer presents a terrace-like morphology similar to the β-Ga_2O_3 substrate but with strong tendency to step bunching. After the deposition of the layers, samples were annealed in a quartz tube at a temperature of 950 °C for 60 min in oxygen ambient. During the annealing step, volatile gallium suboxides are formed which reduce the final layer thickness.

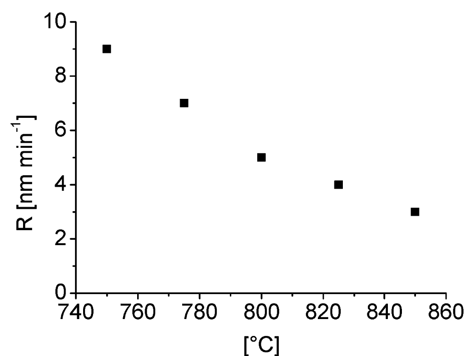

Figure 3 Dependence of the growth rate on the substrate temperature during homoepitaxial growth of β-Ga_2O_3, chamber pressure: 20 mbar.

To determine the structural properties of the β-Ga_2O_3 epitaxial layers, various X-ray diffraction methods were applied. Figure 5 shows an XRD θ–2θ scan of a typical layer. The XRD pattern of the bare β-Ga_2O_3-substrate is also inserted in the graph for comparison.

The X-ray diffraction pattern (θ–2θ-scan) of bare β-Ga_2O_3 substrate (a) is displayed in Fig. 5. The sharp peaks appearing at $2\theta = 14.93°$, 30.08°, 45.80°, and 62.51°can be assigned as the 200, 400, 600, and 800 Bragg reflections of monoclinic β-Ga_2O_3, respectively, in agreement with reported data of β-Ga_2O_3 of the Joint Committee on Powder Diffraction Standards (JCPDS, PDF No. 43043-1012 and 041-1103). The corresponding X-ray diffraction pattern of a β-Ga_2O_3 homoepitaxial layer (b) is also shown in Fig. 5. Again, the 200, 400, 600, and 800 reflections are clearly seen, however, the comparatively weak scattering signal from the Ga_2O_3 layer cannot be separated from the

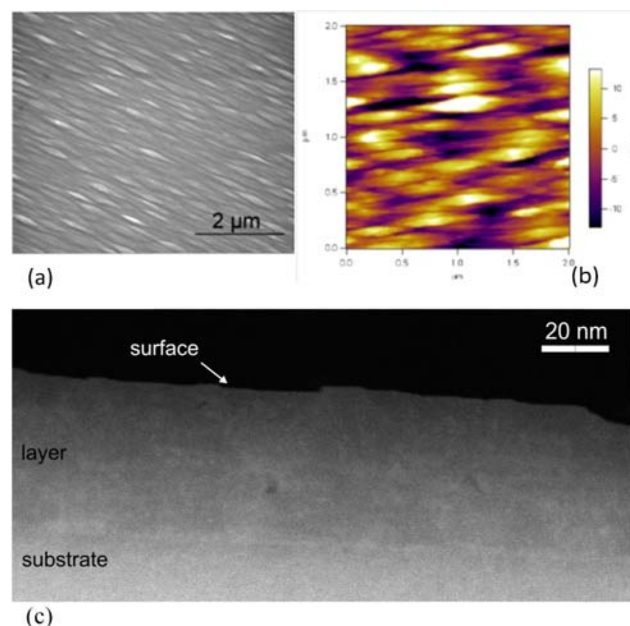

Figure 4 SEM (a), AFM (b), and cross-sectional scanning transmission electron micrograph (c) images of a β-Ga_2O_3 homoepitaxial layer grown at 800 °C and 20 mbar chamber pressure. Layer thickness of about 170 nm, rms: 6.5 nm.

© 2013 WILEY-VCH Verlag GmbH & Co. KGaA, Weinheim

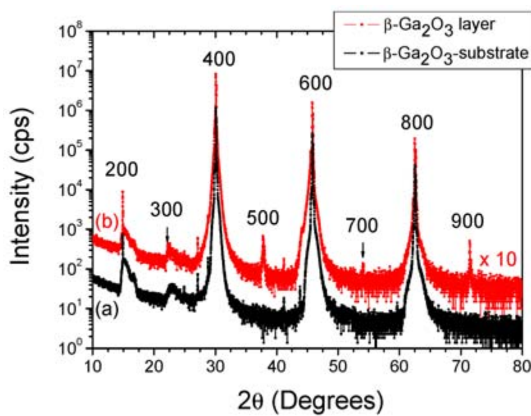

Figure 5 X-ray diffraction pattern (θ–2θ-scan) of (a) bare β-Ga_2O_3-substrate and of a (b) β-Ga_2O_3 homoepitaxial layer deposited at 800 °C. The spectra are vertically shifted by a factor of 10.

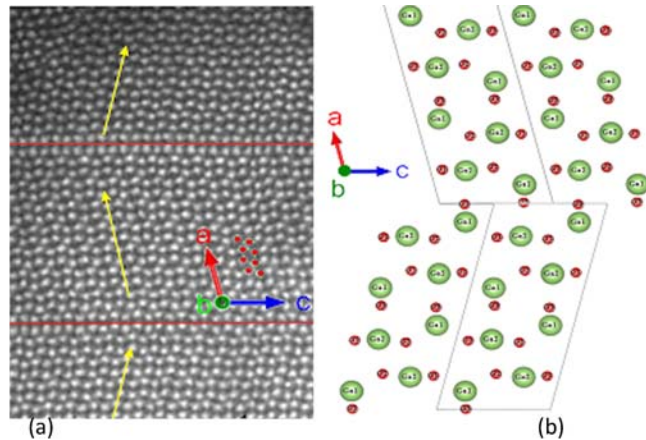

Figure 7 (a) High resolution STEM image of a homoepitaxial grown layer. The orientation shift is marked by the yellow arrows and the stacking fault by the red lines. (b) Structural model of the twin boundary.

strong signal from the substrate. However, in the X-ray diffraction pattern of the Ga_2O_3 homoepitaxial layer additional weak peaks at $2\theta = 22.30°$, $37.77°$, $54.05°$, and $71.47°$ are observed which can be assigned to the odd 300, 500, 700, and 900 reflections, respectively. These Bragg reflections are strictly forbidden for monoclinic β-Ga_2O_3 crystal structure, however, the high density of stacking faults and twins in the epitaxial β-Ga_2O_3 layer that are found in high resolution TEM images (e.g. Fig. 6a) induce strong vertical stacking disorder. This leads to a softening of the X-ray selection rules. The appearance of odd-order Bragg peaks is thus a direct fingerprint of vertical stacking disorder.

Figure 6 shows a typical cross-sectional TEM micrograph of a 150 nm thick (100)-oriented layer grown with water as an oxygen precursor. The layer is coherently grown, but exhibits a high density of stacking faults and twins confirming the results from X-ray diffraction. A typical atomically resolved scanning transmission electron micrograph of a twin boundary in the projection along the *b*-axis, using a high annular angular dark field detector is shown in Fig. 7. Bright dots correspond to gallium columns, while oxygen columns are not visible under these conditions due to their low *Z* compared to Ga. The twin boundary is indicated by a red line. The twin relation can be generated by a c/2 glide reflection of the lattice. Simulations showed a good agreement between these model and the experimental images.

It is well known that annealing under oxidzing atmosphere may have strong influence on structural and electrical properties of oxides. We studied the effect of annealing by high resolution X-ray reciprocal space mapping using the (600) Bragg reflection of β-Ga_2O_3 at 45.80°. Figure 8 shows the scattered intensity distribution around the β-Ga_2O_3 600 reciprocal lattice point for the as-grown β-Ga_2O_3 layer (Fig. 8a) and after annealing in oxygen atmosphere for 1 h at 950 °C (Fig. 8b). The sharp peaks marked as "S" coincide with the 600 reciprocal lattice

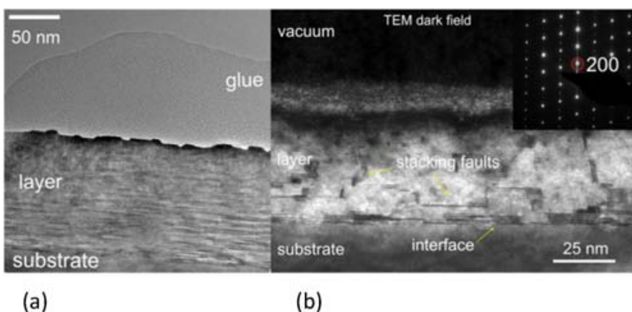

Figure 6 (a) Cross-section multi beam image and (b) dark field TEM image of a Ga_2O_3 layer grown on a Ga_2O_3 substrate.

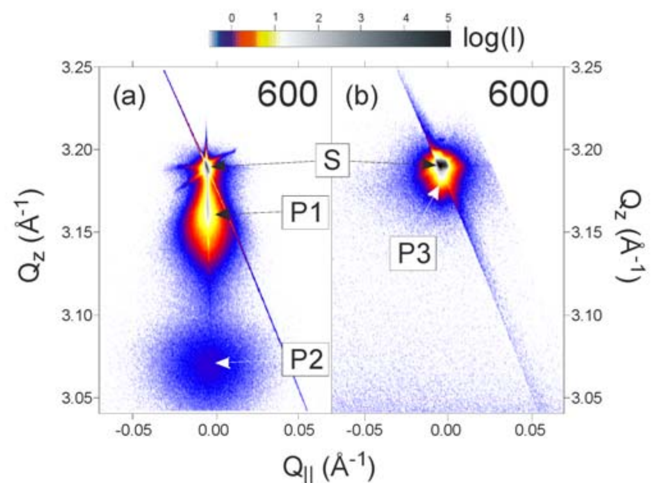

Figure 8 XRD-reciprocal space map in the vicinity of the β-Ga_2O_3 600 reciprocal lattice point (marked as "S") for (a) the as-grown layer and (b) after thermal treatment at 950 °C for 1 h in oxygen. For details see text.

© 2013 WILEY-VCH Verlag GmbH & Co. KGaA, Weinheim

point of β-Ga_2O_3 and derive from the highly perfect Ga_2O_3 substrate. For the as-grown sample two additional weak and broad features P1 and P2 are observed (Fig. 8a) which can be related to the Ga_2O_3 epitaxial layer. The relative position of these features indicate an enhanced vertical lattice spacing of about 0.7% (for P1) and 4.0% (for P2) in the layer as compared to the Ga_2O_3 substrate, while the strong and extended diffuse scattering in the proximity of P1 and P2 is an indication of structural defects in the layer. After a post growth heat treatment, the two features P1 and P2 disappear leaving just a weak shoulder P3 (Fig. 8b) very close to the substrate 600 reflection S.

The observed behavior may have different reasons: (i) a change in the lattice constant due to oxygen vacancies as frequently observed in other oxide compounds, e.g. perovskites [27, 28] or (ii) a reduction in the density of twins and stacking faults. A large stacking fault density indeed implies a large vertical disorder in the diffraction planes of the Ga_2O_3 layer. The disorder usually leads to peak broadening, however, it could also cause changes in the mean vertical lattice spacing and thus lead to comparatively large peaks shifts in X-ray diffraction curves, especially if, as observed in our samples stacking faults have widths, that corresponds to fractions of the unit cell. A similar behavior of peak shift and broadening was observed in (Na, Bi)TiO_3 thin films and could be theoretically described by vertical stacking disorder [26].

Figure 9 shows TEM micrographs of the same sample, i.e. as-grown state and after annealing, under bright field contrast condition. Twinned and undisturbed areas appear as bright and dark contrast in the image. A quantitative analysis of the stacking fault volume by geometrical phase analysis [29] shows that despite the fact that the annealing has led to a decomposition of the layer the total volume of stacking faults and twins reduces. This is promoted by dislocation glide and annihilation through the strain fields of dislocations binding the stacking faults.

Our TEM studies thus corroborate the assumption, confirm that the change in the X-ray data is essentially induced by a reduction in the density of planar defects upon annealing.

Capacitance–voltage (*C*–*V*) and conductivity measurements were performed on as-grown layers and after thermal treatment. Independent of the heat treatment all the layers were highly resistive.

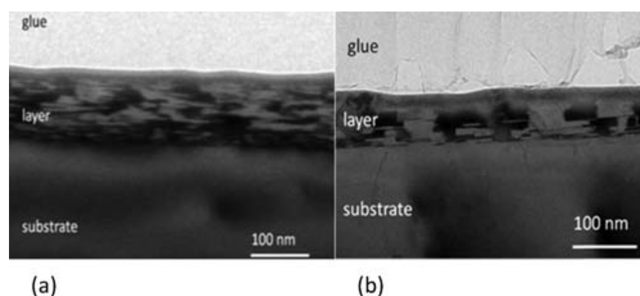

Figure 9 Bright field TEM images of a sample before (a) and after annealing (b) under oxidizing atmosphere at 950 °C.

4 Discussion In the following, we will focus our discussion on the influence of the oxygen precursor on the growth mode. To do so, we briefly summarize our main experimental results: (i) Growth using O_2 as an oxygen precursor proceeds in the form of a thin closed layer, followed by epitaxial growth of whiskers. When moving to extremely oxygen rich conditions, nanocrystalline layers form that have no epitaxial relation to the substrate. (ii) Using H_2O as an oxygen precursor epitaxial growth proceeds in a layer-by-layer mode although the grown layer contains a high density of stacking faults and twins.

To understand the differences, we first analyzed the thermodynamics of the growth atmosphere using the FactSage software package. The calculations were performed for real growth conditions.

Figure 10 shows the amount of main products of the reaction between TMGa and pure oxygen and water, respectively.

When using pure oxygen (Fig. 10a), the main reaction products are solid Ga_2O_3 and gaseous oxygen, water, and carbon dioxide. Other reaction products are at very low concentrations and not shown in the figure (out of scale). For example, $H_2 = 6.7 \times 10^{-13}$ mol, $OH = 7.1 \times 10^{-8}$ mol.

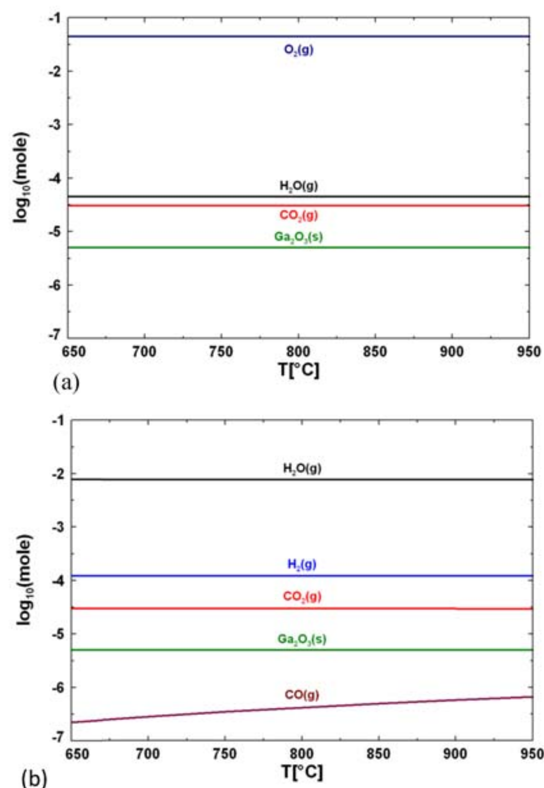

Figure 10 Amount of main species formed during growth of Ga_2O_3 layers when using (a) oxygen and (b) water as oxygen source.

 © 2013 WILEY-VCH Verlag GmbH & Co. KGaA, Weinheim

On the other hand, if water is used as oxygen source (Fig. 10b) then hydrogen molecules, H_2, appear at high concentration as compared with Ga_2O_3 amount, while O_2 molecules are not present at all, since they were fully consumed by organic species.

According to recent literature reports [21, 22, 23], water dissociation and chemisorptions of H^+ on a metal oxide surface can significantly influence the nature of the surface sites, which in turn affects the subsequent adsorption and surface mobility of other molecules. On the other hand, defects like oxygen vacancies can affect the surface chemistry of the Ga_2O_3 surface too. Starting from the thermodynamic considerations, we may now consider the effect of the surface on the absorption and dissociation processes of the growth relevant species. Following the considerations by Pan et al. [20, 25], who performed an in depth experimental and theoretical study on the catalytic action on the (100) surface of Ga_2O_3. In particular, they considered the mutual interaction of H_2O and CO_2 with this surface and the role of oxygen vacancies on the activation of these species. According to their work, H_2O is preferably adsorbed in the form of molecules at the dry surface, producing a hydrated Ga_2O_3 surface, while adsorbed CO_2 is activated and results in a carbonate species in a slightly endothermic reaction. CO_2 if co-adsorbed along with H_2O can be protonated by H_2O and then lead to formation of a bicarbonate. The presence of oxygen vacancies significantly modifies the activity of the surface. CO_2 occupies the oxygen vacancies in an exothermic reaction, while H_2O spontaneously dissociates at the oxygen vacancy side.

Based upon considerations and taking into account our thermodynamical calculations, the influence of the oxygen precursor on the growth mode may be qualitatively discussed as follows. When pure O_2 is employed, the formation energy of oxygen vacancies is substantially increased which in turn lowers their concentration [24]. At the same time, H_2O and CO_2 are present in comparable concentrations, which will promote the formation of $Ga_2(CO_3)_3$ at the growth surface as described above. Such compounds will act as a mask and whiskers will grow out of the unmasked areas. On the other hand when H_2O is employed, the oxygen partial pressure is considerably low and oxygen vacancies are expected to form spontaneously [24]. Since H_2O is present at much higher concentrations than CO_2 the adsorption of CO_2 is prevented and H_2O will spontaneously dissociate at oxygen vacancy sites thus promoting growth. An additional mechanism can also take place: hydrogen may occupy oxygen vacancy sites by forming Ga-H species and reduce the surface state density. As a consequence, the chemical potential of the surface will be more homogeneous and diffusion of desorbed atoms on the surface will be enhanced. Therefore, the relatively high partial pressure of hydrogen deriving from water dissociation could have a positive effect on the kinetics at the substrate surface and hence support the layer-by-layer growth.

5 Conclusions

β-Ga_2O_3 epitaxial layers were grown on β-Ga_2O_3 (100) substrates using MOVPE. Trimethylgallium and pure oxygen or water was used as precursors for gallium and oxygen. With pure oxygen, we are unable to deposit smooth and coherent homoepitaxial layers independently of growth parameters. β-Ga_2O_3 nano-crystals (either wires or agglomerates) were obtained. When using water as oxidant, we succeeded to grow smooth homoepitaxial β-Ga_2O_3 layers. Based on thermodynamical considerations of the gas phase and published *ab initio* data on the catalytic action of the (100) surface of β-Ga_2O_3, we suggested possible mechanisms for the absorption and incorporation processes that result in epitaxial growth. The presence of hydrogen has a positive effect on kinetic conditions of the substrate surface and hence may support the layer-by-layer growth. The structural properties of the β-Ga_2O_3 epitaxial layers were characterized by high resolution XRD diffraction pattern and high resolution transmission electron microscopy. As-grown layers show sharp peaks that were assigned to the monoclinic gallium oxide phase and odd reflections that could be assigned to plane deformation by extended defects. These are essentially stacking faults and twin boundaries as observed. Shifts of the layer XRD peaks towards lower 2θ values with respect to the Bragg reflection for the bulk peaks were observed. After post growth thermal treatment in oxygen-containing atmosphere the reflections of the layers do shift back to the position of the bulk Ga_2O_3 peaks and a reduction of stacking fault density was observed.

Acknowledgements The authors would like to thank to J. Schwarzkopf for fruitful discussion, R. Grüneberg for technical assistance, and A. Kwasnewski for performing the XRD measurements. This work was supported by Grand-No. SAW-2012-IKZ-2 from the Leibniz-Gemeinschaft.

References

[1] E. Fortunato, D. Ginley, H. Hosono, and D. C. Paine, MRS Bull. **32**, 242 (2007).
[2] N. Suzuki, S. Ohira, M. Tanaka, T. Sugawara, K. Nakajima, and T. Shishido, Phys. Status Solidi C **4**, 2310 (2007).
[3] T. J. Marks, J. G. C. Veinot, J. Cui, H. Yan, A. Wang, N. L. Edelman, J. Ni, Q. Huang, D. S. Ginley, and C. Bright, MRS Bull. **25**, 15 (2000).
[4] M. A. Khan, M. Shatalov, H. P. Maruska, H. M. Wang, and E. Kuokstis, Jpn. J. Appl. Phys. **44**, 7191 (2005).
[5] T. Oshima, T. Okuno, N. Arai, N. Suzuki, S. Ohira, and S. Fujita, Appl. Phys. Express **1**, 011202 (2008).
[6] R. Droopad, K. Rajagopalan, J. Abrokwah, L. Adams, N. England, D. Uebelhoer, and P. Fejes, J. Cryst. Growth **301**, 139 (2007).
[7] T. Oshima, T. Okuno, and S. Fujita, Jpn. J. Appl. Phys. **46**, 7217 (2007).
[8] K. Matsuzaki, T. H. Hiramatsu, K. Nomura, H. Yanagi, T. Kamiya, M. Hirano, and H. Hosono, Thin Solid Films **496**, 37 (2006).
[9] M. Holland, C. R. Stanley, W. Reid, R. J. W. Hill, D. A. J. Moran, and I. Thayne, J. Vac. Sci. Technol. B **25**(5), 1706 (2007).

© 2013 WILEY-VCH Verlag GmbH & Co. KGaA, Weinheim

[10] M.-Y. Tsai, O. Bierwagen, M. E. White, and J. S. Speck, J. Vac. Sci. Technol. A **28**, 354 (2010).
[11] M. Orita, H. Ohta, M. Hirano, and H. Hosono, Appl. Phys. Lett. **77**, 4166 (2000).
[12] M. Orita, H. Hiramatsu, H. Ohta, M. Hirano, and H. Hosono, Thin Solid Films **411**, 134 (2002).
[13] M. Ogita, S. Yuasa, K. Kobayashi, Y. Yamada, Y. Nakanishi, and Y. Hatanaka, Appl. Surf. Sci. **212–213**, 397 (2003).
[14] P. Marie, X. Portier, and J. Cardin, Phys. Status Solidi A **205**, 1943 (2008).
[15] H. W. Kim and N. H. Kim, Mater. Sci. Eng. B **110**, 34 (2004).
[16] T. Oshima, N. Arai, N. Suzuki, S. Ohira, and S. Fujita, Thin Solid Films **516**, 5768 (2008).
[17] V. Gottchalch, K. Mergenthaler, G. Wagner, J. Bauer, H. Paetzelt, C. Sturm, and U. Tescher, Phys. Status Solidi A **206**, 2 (2009).
[18] C. Huang, R. Horng, D. Wuu, L. Tu, and H. Kao, Appl. Phys. Lett. **102**, 011119 (2013).
[19] Z. Galazka, R. Uecker, K. Irmscher, M. Albrecht, D. Klimm, M. Pietsch, M. Brützsam, R. Bertram, S. Ganschow, and R. Fornari, Cryst. Res. Technol. **45**, 1229 (2010).
[20] Y. Pan, D. Mei, C. Liu, and Q. Ge, J. Phys. Chem. C **115**, 10140–10146 (2011).
[21] P. Ravadgar, R. H. Horng, and T. Y. Wang, ECS J. Solid State Technol. **1**(4), N58–N60 (2012).
[22] W. Jochum, S. Penner, K. Föttinger, R. Kramer, G. Rupprechter, and B. Klötzer, J. Catal. **256**, 268–277 (2008).
[23] J. B. Varley, H. Peelaers, A. Janotti, and C. G. Van de Walle, J. Phys.: Condens. Matter **23**, 334212 (2011).
[24] G. Luka, M. Godlewski, E. Guziewicz, P. Stakhira, V. Cherpak, and D. Volynyuk, Semicond. Sci. Technol. **27**, 074006 (2012).
[25] Y.-X. Pan, C.-J. Lui, F. Mai, and Q. Ge, Langmuir **26**, 5551 (2010).
[26] V. Kopp, V. Kaganer, J. Schwarzkopf, F. Waidick, T. Remmele, A. Kwasniewski, and M. Schmidbauer, Acta Crystallogr. A **68**, 148 (2012).
[27] Can. Wang, B. L. Cheng, S. Y. Wang, H. B. Lu, Y. L. Zhou, Z. H. Chen, and G. Z. Yang, Thin Solid Films **485**, 82 (2005).
[28] D. A. Freedman, D. Roundy, and T. A. Arias, Phys. Rev. B **80**, 064108 (2009).
[29] R. Schewski, G. Wagner, M. Baldini, D. Gogova, Z. Galazka, M. Schmidbauer, R. Fornari, and M. Albrecht, in preparation.

 © 2013 WILEY-VCH Verlag GmbH & Co. KGaA, Weinheim